Synthetic Lethal Interaction Between *ether-a-go-go Shaker* and *escargot* Mutations in *Drosophila*

Samantha Zhang

Department of Neurobiology and Behavior, Cornell University

Ithaca New York, 14853

Spring 2007

ABSTRACT

Escargot (esg) is a member of the snail family of transcription factors. Gain-of-function *esg* mutantions have been identified in a previous studies as strong suppressors of seizure behavior in *Drosophila* models for epilepsy (Hekmat-Scafe et al. 2005). Recently, during a screen utilizing the *ether-a-go-go (eag) Shaker (Sh)* double mutant to identify genes that affect oxidative stress sensitivity, we uncovered a lethal interaction between gain-of-function *esg* mutations and the *eag Sh* double mutant. The *eag* and *Sh* genes encode potassium channel subunits; epilepsy studies have revealed that *eag* and *Sh* are also mild seizure suppressors (Kuebler et al. 2001). The *esg* gene interaction is thus of great interest as it rescues seizure prone mutations while causing lethality in animals with increased seizure resistance. This study investigates the lethal interaction between *eag Sh* and *esg* to better understand its underlying mechanisms. Our results indicate that lethality is caused by severely impaired motor control in the adult. The animal exhibits many adult specific phenotypes, with distinctive synaptic phenotypes in adult and larvae. These results suggest that the critical period for *esg*-induced lethality is during adult development which agrees with the results of epilepsy studies.

INTRODUCTION

We uncovered a synthetic lethal interaction between the loss of function *ether-a-go-go (eag) Shaker* (*Sh*) double mutant and the gain-of-function neural expression of the transcription factor *escargot (esg)* in *Drosophila melanogaster* through an ongoing genetic screen for genes that affect lifespan and oxidative stress sensitivity. Oxidative stress is of significant health concern as it plays a major role in determining lifespan (Finkel and Holbrook 2000). The *eag Sh* double mutant is hypersensitive to oxidative stress and have a reduced lifespan; thus it was used to identify genes of interest that affect lifespan.

The *eag* and *Sh* mutants are so named for their ether induced leg-shaking phenotype (Kaplan and Trout 1969). The *Sh* gene encodes several types of voltage-gated potassium channel alpha-subunits (Baumann et al 1987; Tempel et al. 1987), resulting in the reduction of I_A potassium current (Salkoff and Wyman 1981). *Eag* encodes a cyclic nucleotide modulated potassium channel subunit (Fergestad et al. 2006) that leads to alterations, but not the loss of four different potassium currents including I_A (Zhong and Wu 1991). Both *Sh* and *eag* mutants experience a reduction in repolarizing current which leads to repetitive firing of action potentials and prolonged

synaptic transmission at the larval neuromuscular junction (NMJ) (Jan et al 1977; Ganetzky and Wu 1982). The resultant hypersensitivity to oxidative free radicals (Trout and Kaplan 1970) promotes the process of senescence and thus reduces lifespan (Finkel and Holbrook 2000).

The double mutant *eag Sh* enhances the phenotype of either of the mutations alone (Ganetzky and Wu 1983). In addition to strengthening the *Sh* phenotypes of leg-shaking under ether anesthesia (Kaplan and Trout 1969) and altered larval locomotion (Wang et al. 2002), the double mutant also exhibit an overgrowth of synaptic innervation at the larval NMJ (Budnik et al. 1990). With a lifespan averaging two weeks as a result of extreme hypersensitivity to oxidative stress, the *eag Sh* combination allows for more dramatic results that expedites the screening process. Repressor lines that suppressed oxidative stress sensitivity were identified, along with lines that had a lethal interaction with *eag Sh.* Of the four lethal lines, three leads to the neuro-overexpression of the gene *escargot (esg).*

The *esg* gene is a member of the snail family of transcription factors that play roles in mesoderm and nervous system development of arthropods and chordates (Manzanares *el al. 2001*). *Esg* is normally expressed in embryonic neuroblasts and contributes to central nervous system (CNS) development (Whiteley et al. 1992; Ashraf et al 1999). The gene encodes a

pr te that er f in ge DNA in mains an gn

th m i A/GCAGGTG (F P 1 A. hraf 99). Th ro in

lud P DL K mai hat ay th dCtBP co pre thi

l gely th ugh f as ma pre f en tran (A hraf

al 99 A hraf as

Th pr f *es* Pl raus any

h types w typ ba km (H km caf al 0:); h v

p pro eral ph types so ated th uronal *ag*

Sh ba kgro d. Th ad lt fly has rely im red or a er al

exh bi um f ad lt spe hen ty Th the th h

res ed fr th *Sh* ynap h type and rt ba k w type

The m tamorphos from h althy arv to

ugg ts tha l pe fi an *ag Sh* te he

pi pe

In gl *Sh* -of-fun m tati h

b ed th pas pr f beha *D ophila*

for ep lepsy H km t- caf l. 00). *Dr ophila* m ta h

as ly ho k d (eas) pr im sy tem w th m th v

kno vn ar easy at aking them ood mod for

ue ll epsy V ed to th gai f-func on

mutations decrease seizure susceptibility by as much as 93% in the progeny with no additional morphological phenotypes observed (Hekmat-Scafe et al. 2005). Yet, when crossed to the *eag Sh* double mutant with an increased threshold for seizure, gain-of-function *esg* interaction results in lethality. This study examines this lethal interaction to gain a better understanding of *esg* gene functions, and gain further insight into the mechanisms that regulate seizure, and affect neuromuscular development.

MATERIALS AND METHODS

Fly Stocks:

TABLE 1 lists the *Drosophila* stocks used in this study. Stocks were raised on standard diet at 25°C. CS-5 is a wild type strain obtained from J Carlson; C155 encodes a neuron-specific Gal4 driver (Lin and Goodman, 1994) and was obtained from Bloomington stock center; *eag Sh* double mutant was acquired from C. F. Wu; the Enhancer P stock (EP) as previously described (Rorth 1996) was obtained from the Szeged *Drosophila* Stock Center in Hungary. Briefly, the EP stock contains genetic insertions of a specialized P-element vector with an upstream activating sequence (UAS) site. Genes downstream of *UAS* can be activated by the transcription factor Gal4. Thus far, 31 EP(2) lines with insertions on the second chromosome were screened in the initial suppressor screen. EP(2) 633, the particular line studied in the synthetic lethal interaction, refers to an EP insertion in the 5' flanking region of the *esg* gene.

Genetic analysis:

C155 and *eag sh* are located on the X chromosome. We combined *C155* with *eag Sh* to drive the expression of genes downstream of the UAS insertion in all neurons (TABLE 1). The presence of the C155 driver was tested by its ability to drive UAS-green florescence protein (UAS-GFP); the presence of *eag Sh* was tested from behavioral observation of ether induced shaking. The *C155 eag Sh* line was balanced over FM7i, which carried an insertion of *ubiquitous*-GFP, and *Bar*. This allowed us to identify larval and adult genotypes of interest by the absence of GFP in larvae and absence of bar-shaped eyes in adults. Throughout this study, the genotype of *elav-Gal4^{C155} eag Sh^{120}/ Fm7i-B GFP* is referred to as C155 *eag Sh* . In the screen for *eag Sh* phenotype suppressors, males from each EP(2) line were crossed to C155 *eag Sh* females (FIGURE 1). The EP insertions were either homozygous or balanced over *Curly-of-Oster (Cyo)*. The resultant F1 male progeny of interest would therefore have non-curly wings, and a genotype of *elav-Gal4^{C155} eag Sh^{120}/Y; EP(2)/+*. For *esg* in particular, F1 progeny with the genotype *elav-Gal4^{C155} eag Sh^{120}/Y(+); esg^{EP633}/+* were referred to as ***C155 eag Sh; esg^{EP}*** throughout this study

When making crosses, flies were anesthetized under CO_2, sorted, and put into vials with standard diet. Each vial contained six virgin females and

six males of appropriate genotype. Flies were transferred to a new vial every other day to create vials of larval and adult cultures that will reach various stages of development in succession. For the *C155 eag Sh; esg*^{EP} mutant, the vials were inverted before the flies eclosed; this allowed the flies to fall away from food and be collected for this study.

Behavioral Testing:

For ether testing, adult flies were collected and exposed to ether for 30 sec using an etherizer from Carolina Biological, and observed under a microscope for leg-shaking behavior.

Paraquat was used to test for oxidative-stress sensitivity in 2-4 day old flies (as described in Wang et al. 2002). F males with non-bar eyes from the *C155 eag Sh, EP* crosses were fed 20mM paraquat in 4% sucrose, and lifespan was monitored for 48 hours. Nearly all wild type flies survive paraquat feeding, whereas about 10% of *C155 eag Sh* flies survive. We identified suppressors as those EP lines that when crossed to *C155 eag Sh,* produce F1 flies with ≥ 40% survivorship after paraquat feeding. Certain lines did not produce viable non-bar eyed F males to be placed under paraquat for oxidative-stress sensitivity testing; these lines were identified as synthetic lethals.

Immunocytochemistry and Microscopy

Third instar wandering larvae (FIGURE 2) and adult abdomens were dissected as described in Stewart et al. (1994) and Rivlin et al. (2004). Specimens were fixed in 3.5% paraformaldehyde and processed for immunocytochemistry as described in Rivlin et al. (2004). Briefly, specimens were blocked in normal sera, incubated in primary antibody overnight, rinsed and incubated in secondary antibody for 2h at room temperature, rinsed and mounted on slides. Antibodies used included anti-fasciclin II (α--FasII) at :50 (Hybridoma Developmental Bank); anti-disc large (α-DLG) at :500 (Hybridoma Developmental Bank); Cy3-conjugated anti-horseradish peroxidase (α-HRP) at 1:200 (Jackson Immunochemicals, Inc.). Alexa 488-conjugated secondary antibodies (Molecular Probes, Inc.) were used at 1:500. In some cases, muscles were also stained with fluorescent phalloidin (Molecular Probes, Inc.) which labels filamentous actin. Stained larval and adult preparations were viewed with a Leica Confocal Microscope. Adult bisections were viewed with a Zeiss AxoskopII microscope.

Bouton counts.

Larval preparations were incubated in rabbit anti-synaptotagmin (provided by N. Reist) and processed using a Vectastain Elite ABC kit (Vector Laboratories, Inc.). The larvae preps were then permanently stained with 3,3'-diaminobenzidine (DAB). The number of anti-synaptotagmin labeled boutons was counted on muscles 6 and 7 in the 3rd abdominal segment (FIGURE 3). Muscle length and width were measured using an optical micrometer. Bouton density was calculated as number of boutons per μm^2

Mean *C155 eag Sh*: 0.194, Std Dev *C155 eag Sh*: 0.0248, n = 16; Mean *C155 eag Sh; esg^{EP}*: 0.120, Std Dev *C155 eag Sh; esg^{EP}*: 0.0232, n = 16).

Using T-test: $\sigma_d^2 = \frac{\sigma_1^2}{n} + \frac{\sigma_1^2}{n} = \frac{.0248560052^2}{16} + \frac{.02322322^2}{16}$

$\sigma_d = .008504$

$$t = \frac{\bar{X}_1 + \bar{X}_2}{\sigma_d} = \frac{0.19433325 - 0.12094293}{.008504} = 8.63009$$

Critical t value from table ($n_1+n_2 - 2$ degrees of freedom) = 3.65 (for $p < .001$)

Adult whole-mounts.

To visualize the flight musculature, adult flies were fixed in 3.5% paraformaldehyde in PBS overnight and bisected. Hemi-fly preparations were dehydrated in ethanol, cleared in methyl salicylate and mounted on slides. Slides were viewed on a Zeiss AxoskopII microscope.

To visualize legs, animals were chilled on ice and legs were severed through the coxa. Legs were imaged with a Leica MZFLIII stereoscope and Leica MF500 digital camera.

RESULTS

Screen for genes that effect *C155 eag Sh120* reveals esg^{EP} as a synthetic lethal enhancer.

In an ongoing lifespan study, Drosophila EP lines were screened through paraquat feeding to identify neuronally expressed genes that would reduce oxidative stress sensitivity and increase lifespan of the short-lived *eag Sh120* mutant. The mean survivorship for *eag Sh* was 14.9 ± 0.5% (n 973) after paraquat feeding. A screen of 331 EP insertions on the second chromosome revealed 23 lines of interest (TABLE 2): these include 19 suppressor and 4 synthetic lethal lines. Suppressor crosses that produced F flies with greater than 40 percent survival after paraquat feeding include EP insertions in genes that encode the transcription factors *mef2* and *lola*, and the anti-oxidant gene, *glutathione S transferase*.

Of the synthetic lethal lines, the previously undescribed gene after the EP(2)627 insertion consists of a genetic sequence that suggests trypsin-like activity. The other lethal lines, EP633, EP684 and EP2009, are all insertions before the *esg* gene. Previous publication shows that these esg^{EP} lines exhibit no mutant phenotype when driven with *C155 gal4* in a wild type background (Hekmat-Scafe et al. 2005). All three of these esg^{EP} insertions

th flank eg f th ge on he ar

oc rs :h flankin f ut :h w sy :th

:h ti ty th *C155* d/ b rte th po te

en f th the in GAL4 :h l to

tr (H kmat f 00 ef y d

har Pri in :h te on be ar l :h

m to h *C155* *Sh* (ty

G l4^{C} *Sh es* +)

F te ogy f *ag Sh, esg*

Th *C155* *Sh* m tan l FP from the pal

an :h ul tage in l m H we co tr l ly

mpaired al h examined bo h fem M ta

p be in d ha littl f h l FP$_d$ h

ry :h body (F GURE 4 Th hak :h f

h th the haking h type be ng er :h m th :h

f al Th m femur tw ed :h rt, h th f tan

morph lly a l type Upo spec th fem ur

m f he tan m l be ab GURE

After eclosion, the fly falls from the pupal case and remains on its back and side, unable to erect itself. Wing-buzzing behavior was observed in the female, but no flight occurs. Bisection of the adult thorax along the sagittal plane showed that the dorsal longitudinal muscles (DLM) are fully developed (FIGURE 6). Due to its drastically impaired motor functions, the *C155 eag Sh; esg^{EP}* adult is unable to maneuver in its food: if left alone, the mutant would either starve or be asphyxiated in the food within 48 to 72 hours after eclosion.

C155 eag Sh; esg^{EP} flies also exhibit an eye phenotype (FIGURE 7). While C155 *eag Sh* flies have large oval wild type-like eyes, all *C155 eag Sh; esg^{EP}* mutants exhibit ateardrop shaped eye that increases in deviation towards the ventral portion. These eyes consist of fewer ommatidia with abnormal pigmentation. In the wild type fly, the mechanosensory bristles between the ommatidia are spread through out the eye; in *C155 eag Sh, esg^{EP}*, the bristles are confined to a small patch at the dorsal portion of the eye, and the orbital bristles surrounding the eye sockets are stunted in growth.

Synaptic phenotype at the NMJ.

Impaired adult motor function may be due to abnormal neuromuscular development. To address this question, the morphology of the muscles and synapses in adult and larvae were analyzed. Qualitative examination of the adult abdominal NMJ was performed to distinguish the effect of neuronal esg^{EP} on the synaptic phenotype of *eag Sh* in comparison to *eag Sh* alone. Adult abdomens were dissected and stained with phalloidin and α-HRP (FIGURE 8). Phalloidin binds to filamentous actin and was used to stain muscles, while α-HRP was used to label all neural membranes (Sun and Salvaterra 1995). In the *C155 eag Sh; esg*^{EP} adult preps, it was noted that α-HRP labeled both neurons and muscles. Using Photoshop, double-labeled portions were channeled away and the image contrast increased to accentuate synaptic visualization. The ventral and lateral muscles of the fourth abdominal section were inspected alone with an overview of the whole adult abdomen prep. While the overview and the ventral NMJ showed little difference between the mutants, there appeared to be a decrease in anti-HRP staining at the lateral NMJ of *C155 eag Sh; esg*^{EP} This reduction appeared to be more severe in the male than the female.

Larval muscles 6 and 7 were examined to quantitatively compare synaptic development between *C155 eag Sh* and *C155 eag Sh; esg*^{EP} An example overview of the synaptic phenotypes in *C155 eag Sh, C155 eag Sh;*

:he tv tr :l: C: g^E: :h in F GURE Anti-
D L ge (DLG v spe fi: ally l: bel bo ton and HRP th
:urons DLG erv ffol prote :h type glutam ter
sy ps :h: :h: :h: :l: di ts :ynap truct (B dn k,
9). Th: assoc te type bo arg and DLP he
m:m an :urroun :h bo (Lah :y 1 :4). N: iffe: enc
bLG stainin; :rved :tw: m: tan :tr
H: th: :h: pe f th: NMJ pears to be iffer C
tr :mpar *C155 ag :h* an *C155 ag Sh* m: tan
(F GURE 6 :h :h h: m: pread N MJ While :hi: ay fl
ffe enc bo ton ty v bey th: scope f h: ct to
q α :ify to

Sh m: tants :ul: ergr th f :h: sy bout: :h:
:rv :l NMJ (dnik al 90). W th: refar ted he um f
bo ton the larv :l NMJ to term f uronal *es* :nh: ed th:
sy h: ype f *Sh* bouton cour :in; th: pr ps wer
pe ly tai :h DAB d GURE Th: to er ab :l:
v :th :y aptotagm syt Sy f: y f m: bra e-erffi:k:ng
pr te ns an C :ynap :l: prote (
00). l: ll bout: type w: fo ge :l cation f

bouton regardless of size. The results of bouton density are presented in FIGURE 11. Bouton density of esg^{EP} (n=12) is not significantly different from the wild type CS-5 (n=12), while *C155 eag Sh* (n=12) is significantly higher than wild type. Surprisingly, bouton density of *C155 eag Sh;* esg^{EP} (n=18) is significantly lower than that of *C155 eag Sh* ($p<0.01$), thus suggesting that neuronal esg^{EP} reverts or rescues the *C155 eag Sh* synaptic phenotype.

DISCUSSION

Synthetic lethality

Ectopic expression of neuronal *esg* in a wildtype background is not associated with any obvious morphological or behavioral phenotypes (Hekmat-Scafe et al. 2004). The exhibition of dramatic phenotype specific for the triple mutant shows that the *eag Sh* and esg^{EP} interaction is truly a synthetic lethal one. The lethality of all three tested esg^{EP} crosses with independently derived P-element insertions reinforces the presence of a synthetic lethal interaction between *eag Sh* and *esg*. One other esg^{EP} insertion, EP683, also occurs in the 5'-flanking region of *esg* but showed no synthetic lethal activity with C155 eag Sh. However, since EP683 is inserted in the opposite orientation of the other esg^{EP} lines, GAL4 induction should not lead to *esg* transcription, and as expected, does not result in a lethal interaction (Hekmat-Scafe et al. 2005). It is noteworthy that neuronal *esg* causes lethality even in females that are heterozygous for *eag Sh*.

We hypothesize that neuronal *esg* acts as a lethal enhancer of oxidative stress sensitivity. While suppressor lines from the screen serve to increase oxidative stress resistance in *eag Sh* mutants; it is likely that "enhancers" are lethal due to the increased sensitivity to oxidative stress. In

the case of the lethal mutants such as *esg*, oxidative stress sensitivity could not be tested due to the detrimental effects of the mutant phenotype. However, unlike *eag Sh*, *C155 eag Sh; esg*^{EP} mutants exhibit moderate leg shaking even in the absence of ether and shake vigorously under carbon dioxide, thus signifying a heightened sensitivity to oxidative stress. While the synthetic lethality comes about as a result of motor function failure, which shall be further studied, the interaction itself is very interesting as both neuroally driven *esg* and the eag and *Sh* mutantions are known seizure suppressors. Such synthetic interaction raises questions of levels of expression in which while a certain amount of phenotypic expression would promote the health of an animal, here a threshold was crossed in which the high level of seizure suppressing phenotypes resulted in a nonviable animal. *esg*, being a transcription factor, affects many aspects of adult development that is yet to be understood. Thankfully, the transcriptional targets of *esg* have been identified through microarray analysis, and the possible interaction of these targets with the *Sh* mutation could be further studied to gain an insight into the process of seizure suppression.

***eag*, *Sh* and *neuronal esg* are seizure suppressors**

Both *eag* and *Sh* are mild suppressors of seizure in *Drosophila* "epilepsy" mutants (Kuebler et al. 2001), while neuronal *esg* acts as a highly effective seizure suppressor gene, reducing the effect of *easily-shocked (eas)* seizure model mutation by as much as 93 percent (Hekmat-Scafe et al. 2004). Time-course experiments have revealed that neuronal *esg* must be expressed during the pupal development of the nervous system for it to act as a gain-of-function seizure suppressor (Hekmat-Scafe et al. 2004). Since the biological functions of *esg* are not obviously associated to electrical excitability, its seizure suppressing abilities and its interaction with *eag* and *Sh* seems to be linked to nervous system development.

Hekmat-Scafe et al (2004) suggested that *esg* increases seizure threshold of epilepsy mutants by acting on postmitotic larval neurons that differentiate into adult CNS interneurons. When neuronal *esg* is expressed in "epilepsy" mutants such as *easily shocked* or wildtype, progeny are not only viable but have increased seizure threshold. Our study of the synthetic lethal interaction between the three seizure suppressors, *eag*, *Sh* and esg^{EP} may provide new insights into the mechanism of seizures, and ultimately lead to development of anti-epileptic drugs with minimum toxic side effects.

Muscular phenotype

Phalloidin staining of larval bodywall preps showed no obvious muscle phenotype for the *eag Sh; esg* (FIGURE 9). Furthermore, the presence of adult mutant progeny showed that the pupal "eclosion" muscles (Kimura 1990) are operational in the *eag Sh; esg* mutant. Only adult specific muscles may be impaired (i.e. legs). Again, this suggests that neuronal *esg* affects adult neurons more than larval derived neurons.

C155 eag Sh; esg^{EP} males display a "twisted" femur phenotype, which is not observed in females which are heterozygous for *eag Sh*. Because *esg* is driven in the nervous system we suggest that the twisted leg phenotype may be due to hyperactivation of leg muscles. Adult muscles require innervation for proper growth and differentiation (fernandes et al. 2001). At a gross level, we did not observe any effects on the growth of the largest muscles in the fly, the indirect flight muscles, thus suggesting that muscle-nerve interactions that are necessary for proper muscle development are not disrupted. Instead we suggest that the apparent twisting of the femur muscle may be due to hyperactivity in the innervating motor neuron. Note this phenotype is not seen in *eag sh* mutants at this age, but hypercontraction of muscles, particularly the flight muscles, is observed in some *sh* mutants as they age (i.e. Wings down phenotype; unpublished results, p. Rivlin).

Neuromuscular Junction

Our results suggest that neuronal *esg* can rescue the synaptic overgrowth phenotype of *eag Sh* larvae (Budnik et al. 1990). This was unexpected given that neuronal *esg* appears to act as an enhancer of the leg shaking phenotype. We also conducted a preliminary investigation of the adult abdominal NMJ of the triple mutant. As in the larva, *eag Sh* results in increased innervation at the adult abdominal NMJ (Hebbar et al. 2006). In the *eag Sh; esg* adult preps, α-HRP immunoreactivity was prevalent in both the neurons and the muscles. Specifically, the horseradish peroxidase recognizes an epitope that is expressed on all neural membranes. Sun and Salvaterrra (1995) identified the α-HRP epitope as sodium potassium ATPase encoded by the gene *nervana 1*. A second form of *nervana* is also expressed on muscles; we suggest that the increased α-HRP immunoreactivity may be due to increased expression of nervana in mutant muscles. The other possibility is that the phalloidin labeling was too bright and resulted in a high background for α-HRP. However, since *eag Sh* preps prepared in the same trial did not display the same background noise, this suggests that the increased staining is due to increase in α-HRP immunoreactivity.

Aside from the NMJ observations, the presence of the eye and bristle phenotype also denotes an disruption in neural development of the adult. Further discussion of the phenotype is provided below.

Eye phenotype

The *eag Sh; esg* mutant eye phenotype is of great interest. Based on the eye's teardrop shape, the mutant phenotype seems to result from developmental defects. In the triple mutant, the anterior portion of the eye is similar to wild type, and mechanosensory bristles are present between the ommatidia (FIGURE 7). However, after a certain point towards the posterior region, the number of ommatidia decreases dramatically and the bristles are no longer present. The abnormal mechenosensory bristles around the eye also show developmental defects as the bristles are stunted in growth. While little previous work has been done on the development of bristles in *Drosophila,* the compound eye develops from the posterior to the anterior depending on the movement of a morphogenetic furrow (MF) on the eye imaginal disc (Bessa et al. 2002). Early *Drosophila* eye development is not well understood, but by determining the onset time of *esg* gene expression, the *eag Sh; esg* mutant may be used as a model to map out ommatidial patterning and cell communication in the developing eye.

In the next stage of this research project, heat inducible Gal4 will be crossed to *eag Sh* so that the neuronal expression of *esg* can be induced at various stages of development by exposure to high temperature. The eye phenotype of the resultant progeny will be crucial in determining the role of *esg* and *eag Sh* in ocular development by examining the point in which ommatidia reduction occurs. Other mutant phenotypes as described in this study will also be monitored to examine the full developmental effect of the synthetic lethal interaction.

Synaptic phenotype

Our results suggest that adult lethality results from impaired motor function. Perhaps the most interesting finding is that neuronal esg appears to rescue the synaptic overgrowth phenotype of *eag Sh* larvae. While additional data must be collected, it appears that neuronal *esg* does not have a similar effect in the adult, as evidenced by the diminished anti-HRP staining at the lateral abdominal adult NMJ (FIGURE 8). This may reflect a more severe, dysfunctional synaptic phenotype than *eag Sh* alone. Our results suggest that *C155 eag Sh; esg*^{EP} has a more severe effect on the adult stage than the larval stage. It is possible that the larva possesses the ability to

compensate for any detrimental effects of neuronal esg, whereas the adult is more vulnerable.

It is noteworthy that this parallels the findings of Hekmat-Scafe et al. (2005) which suggest that seizure suppression by neuronal *esg* is not due to its effects in larval neurons, but rather its effects in adult-specific neurons A very interestingly possibility is that the same population of neurons play a critical role in seizure sensitivity and the lethal interaction studied here. It will be interesting in the future to use GAL4 drivers specific to different types of neurons, such as interneurons and motor neurons to see if the lethal effects of esg^{EP} are specific to a certain subset of adult neurons. In addition, it will be interesting to extend this study to look at other *Sh* alleles

LITERATURE CITED

Ashraf SS, Sochacka E, Cain R, Guenther R, Malkiewicz A, Agris P. 1999. Single atom modification (O->S) of tRNA confers ribosome binding. RNA 5: 188-194.

Ashraf SI, Ip YT. 2001. The Snail protein family regulates neuroblast expression of inscuteable and string, genes involved in asymmetry and cell division in Drosophila. Development 128: 4757-4767

Baumann G, Stolar MW, Amburn K, Barsano CP, DeVries BCJ. 1987. din. Endocr. Metab. 62: 134-141

Budnik V, Zhong Y, Wu C-F (1990) Morphological plasticity of motor axon terminals in Drosophila mutants with altered excitability. J Neurosci 10: 3754-3768 .

Chau YP, Lu KS. 1995. Investigation of the blood-ganglion barrier properties in rat sympathetic ganglia by using lanthanum ion and horseradish peroxidase as tracers. ACTA ANATOMICA (BASEL) 153 (2). 135-144.

Coyle JT, Puttfarcken P. Oxidative stress, glutamate, and neurodegenerative disorders Science 262, Issue 5134, 689-695.

Dobzhansky, T. 1946. Genetics of natural populations. XIII. Recombination and variability in populations of Drosophila pseudoobscura. Genetics 31, 269-290.

Fergestad et al. 2006. Neuropathology in Drosophila membrane excitability mutants. Genetics 172(2). 1031—1042.

Finkel T, Holbrook NJ. 2000. Oxidants, oxidative stress and the biology of ageing. Nature 408, 239-247.

Fuse NK, Yasumoto H, Suzuki, K, Takahashi, Shibahara S. 1996. Identification of a melanocyte-type promoter of the microphthalmia-associated transcription factor gene. Biochem. Biophys. Res. Commun. 219. 702-707

Ganetzky B, Wu CF. 1983. Neurogenetic analysis of potassium crrents in Drosophila: Synergistic effects on neuromuscular transmission in double mutants. J. Neurogenet. 1 17-28

Hartman JL t. et al. 2001 Principles for the buffering of genetic variation. Science 291: 1001-1004.

Hekmat-Scafe DS, Dang KN, Tanouye MA. 2005. Seizure suppression by gain-of-function escargot mutations. Genetics 169: 1477-1493.

Jan YN, Jan LY, Dennis MJ. 1977. Two mutations of synaptic transmission in Drosophila Proc. R. Soc. London 198: 87-108

Kaplan WD, Trout WE. 1969. The behavior of four neurological mutants on Drosophila. Genetics 61, 399-409

Lehninger Principles of Biochemistry, Fourth Edition,

Lin DM, Goodman CS. 1994. Ectopic and increased expressin of fasciclin II alters motoneuron growth cone guidance. Neuron 13: 507-523.

Lucchesi, J 1967, Synthetic lethality and semi-lethality among functionally related mutants of Drosophila melanogaster. Genetics 59: 37—44.

Manzanares M, Locascio A, Nieto MA. 2001. The increasing complexity of the Snail gene superfamily in metazoan evolution. Trends in Genetics 17: 178-181.

Pavlidis P, Tanouye MA. 1994. Seizures and failures in the giant fiber pathway of Drosophila bang-sensitive paralytic mutants. Journal of Neuroscience 15: 5810-5819.

Pang ZP, Melicoff E, Padgett D, Liu Y, Teich AF, Dickey BF, et al. 2006. Synaptotagmin-2 is essential for survival and contributes to Ca^{2+} triggering of neurotransmitter release in central and neuromuscular synapses. The Journal of Neuroscience 26: 13493-13504.

Rivlin J, Mendel J, Rubinstein S, Etkovitz N, Breitbart H. 2004. Role of hydrogen peroxide in sperm capacitation and acrosome reaction. Biology of Reproduction 70: 518–522

Rorth P. 1996. A modular misexpression screen in Drosophila detecting tissue-specific phenotypes. National acad sciences 93: 12418-12422.

Salkoff L, Wyman R. 1981. Genetic modificatin of potassium channels in drosophila shaker mutants. Nature 293: 288-230.

Stewart BA, Atwood HL, Renger JJ, Wang J, Wu C-F. 1994. Improved stability of Drosophila larval neuromuscular preparations in haemolymph-like physiological solutions. J Comp Physiol 175:179-191.

Tempel BL, Jan YN, Jan LY. 1988. Cloning of a probable potassium channel gene from mouse brain. Nature 332: 837-839.

TABLES AND FIGURES

TABLE 1. *Drosophila* Stocks

Stock	Genotype
CS-5	*wildtype*
C155	*elav-Gal4^{C155}*
eag Sh	*eag Sh^{120}/ Fm7i-Bar, ubi-GFP*
EP(2)	*w; insertion^{EP} /Cyo or w; insertion^{EP} / insertion^{EP}*
esg^{EP}	*w; esg^{EP633}/ esg^{EP633}*
C155 eag sh	*elav-Gal4^{C155} eag Sh^{120}/ Fm7i-B GFP*
C155 eag sh; esg^{EP}	*elav-Gal4^{C155} eag Sh^{120}; esg^{EP633}*

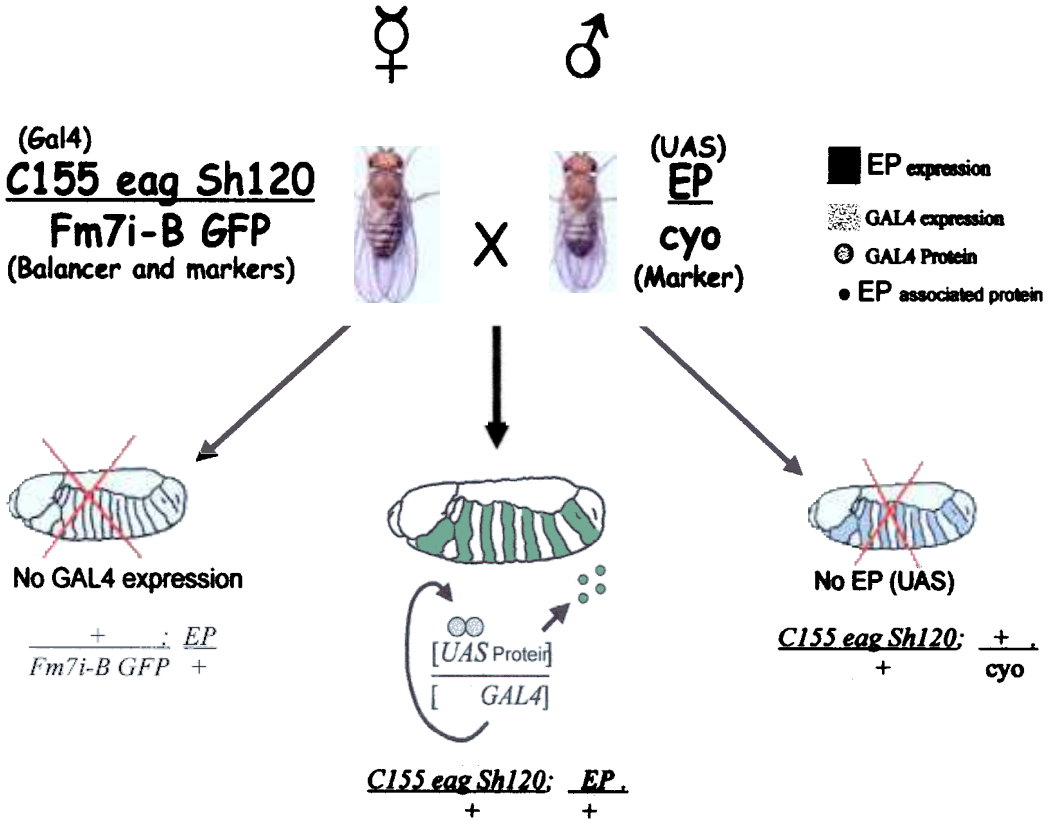

FIGURE 1. *C155 eag Sh* and *EP* cross

Virgin female flies carrying the recombinant X-chromosome *elav-gal4* ^{C155} *eag Sh* and the balancer chromosome, FM7i (which is marked with GFP and bar eyed) were crossed with males carrying a UAS-bearing EP insertion balanced over *Cyo* (*curly* marker). EP insertions on the second chromosome were examined in this study. Male F1 progeny that were hemizyogous for *elav-Gal4*^{C155} *eag Sh* and contained one copy of UAS-bearing EP insertion were selected for study.

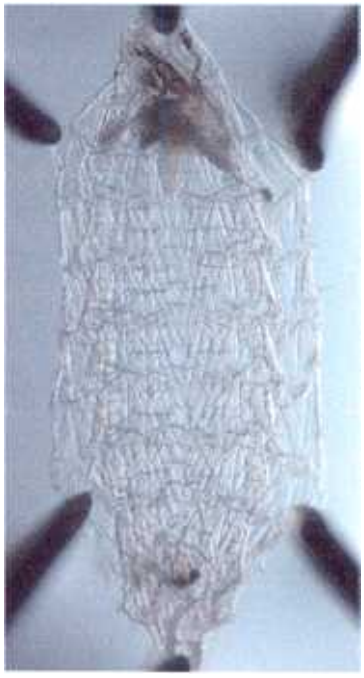

FIGURE 2. *Drosophila* larval prep
Third instar larvae were filleted in a magnetic dissecting dish. The prep was spread out as seen with magnetic pins. The larval muscles were visible along with the brain and ganglion located at the top of the prep.

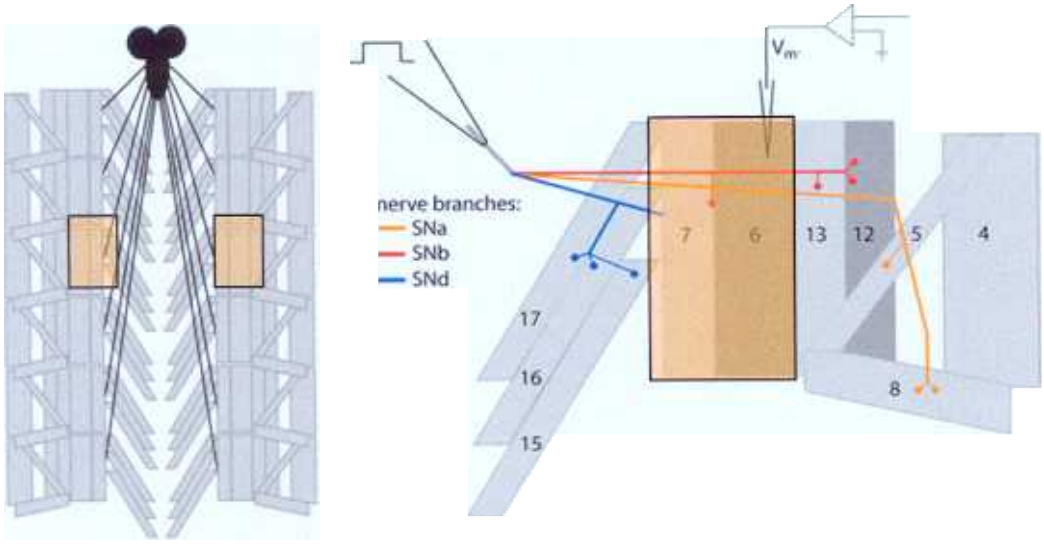

FIGURE 3. Larval muscle layout
Diagram of *Drosophila* larvae prep labels the muscles and perspective nerves that innervate each segment. For bouton density, boutons were counted from muscles 6 and 7 of the 3rd segment from the anterior end of the third instar wandering stage larvae (see colored segment).

From Hoy Lab website

TABLE 2. EP(2) screen

EP line suppressors	Gene	% survival	EP line lethals	Gene
EP(2)315	Unknown	65.5	EP627	Unknown
EP(2)316	Unknown	48.8	EP633	*escargot (esg)*
EP(2)330	Unknown	51.3	EP684	*escargot (esg)*
EP(2)337	GSTS1	80.5	EP2009	*escargot (esg)*
EP(2)340	Unknown	73.3		
EP(2)343	Unknown	47.5		
EP(2)348	Unknown	60.6		
EP(2)349	Unknown	50		
EP(2)354	lola	87.9		
EP(2)372	CG4738	54.4		
EP(2)397	chic	52		
EP(2)479	mef2	47		
EP(2)493	l(2)02045	51		
EP(2)531	CG13434	47		
EP(2)548	CG6751	44		
EP(2)608	E(Pc)	46		
EP(2)683	Unknown	41		
EP(2)938	Unknown	42		
EP(2)1236	GSTS1	47		

The results to date of the screen for second chromosome Enhancer P (EP(2)) mutations that suppress oxidative stress sensitivity of *eag Sh* are presented. The flies tested were males of genotype *elav-Gal4^{C155} eag Sh/y; EP/+*. They resulted from crosses between *elav-Gal4^{C155} eag Sh/FM7i-B GFP* virgin females and *w; EP/Cyo* males. Control flies of genotype *elav-Gal4^{C155} eag Sh/y* were used; after paraquat feeding, their mean percent survival was 14.9 ± 0.5% (n = 973). Suppressor lines were defined as crosses with mean percent survival ≥40%. Lethal lines were those that produced non-viable progeny in the cross. When known, the corresponding gene is noted.

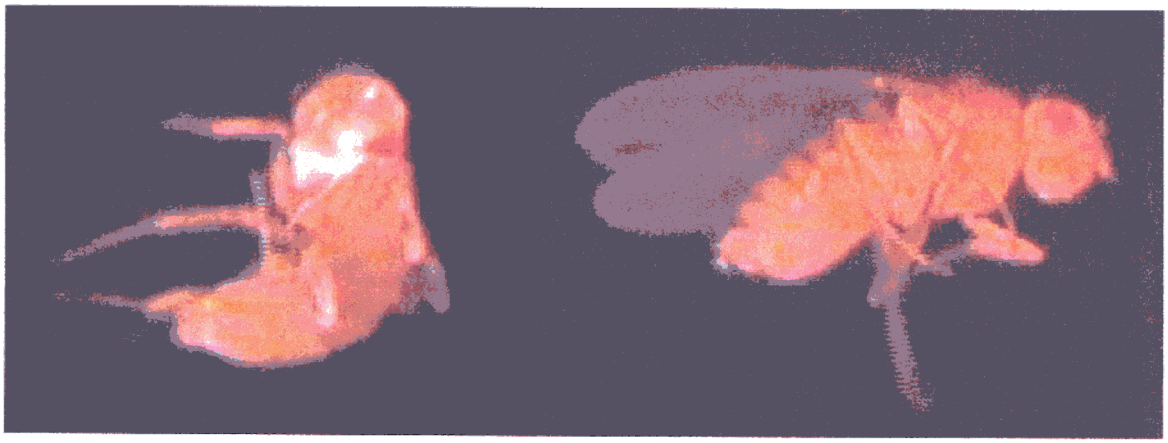

MALE
elav-Gal4^{C155} *eag Sh*^{120}*/Y; esg*^{EP633}*/+*

FEMALE
elav-Gal4^{C155} *eag Sh*^{120}*/+; esg*^{EP633}*/+*

FIGURE 4. C155 *eag Sh; esg*^{EP} adult
The adult mutant exhibits severe motor function impairments. The leg muscles of both male and female fly are contracted and shake in the absence of ether. These flies are unable to stand, and remain laying on their side or back. Their lifespan is about 48 to 72 hours after eclosion.

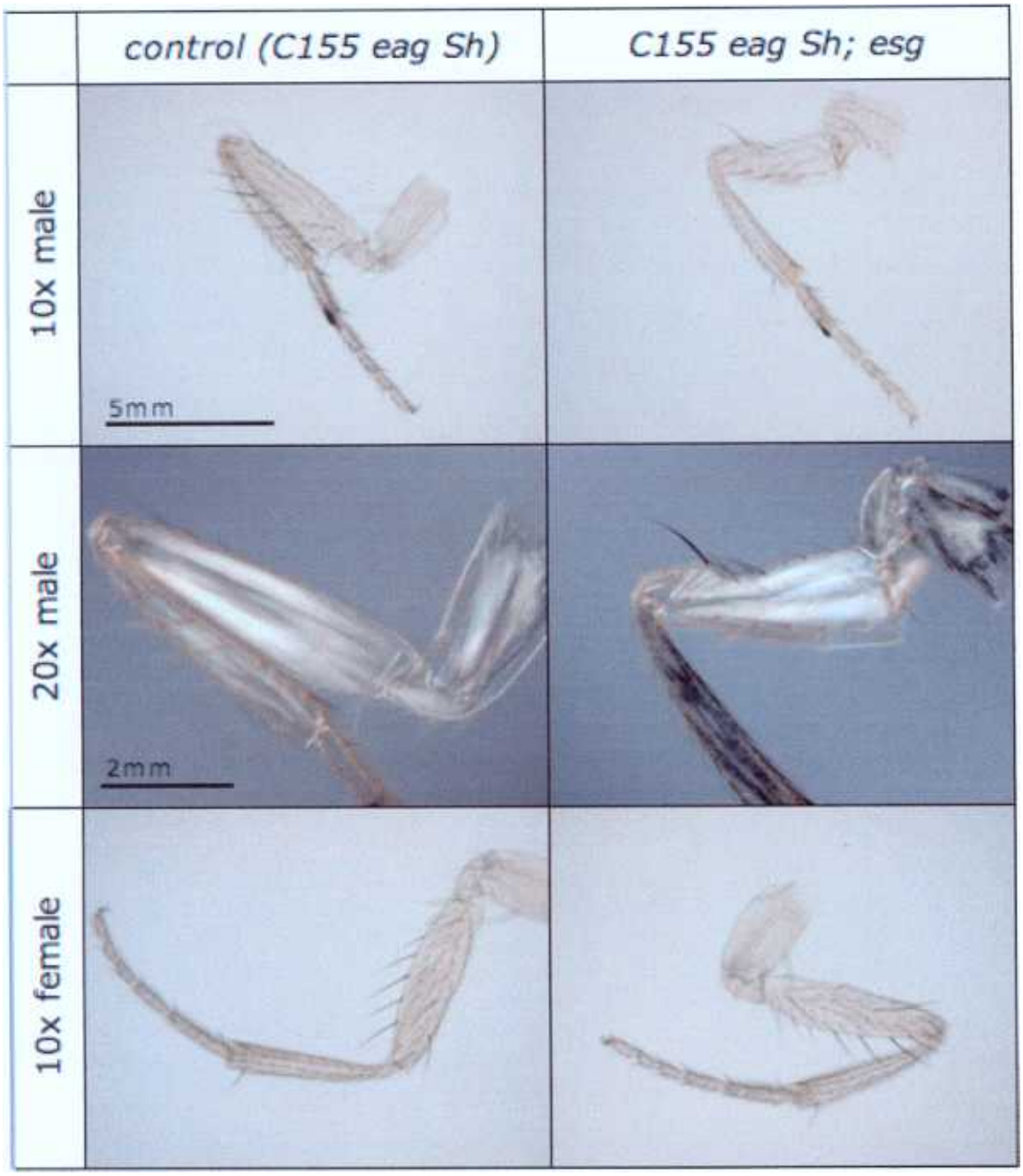

FIGURE 5. Mutant leg phenotype
Digital camera (10x) and stereoscope (20x) images of wild type and *C155 eag Sh; esg^{EP}* mutant legs are presented. Scale bars for 10x and 20x magnification are given. The control legs are those of *C155 eag Sh*, which exhibits wild type leg phenotype. The 10x image shows external bristles while the stereoscope image shows internal muscle structure.

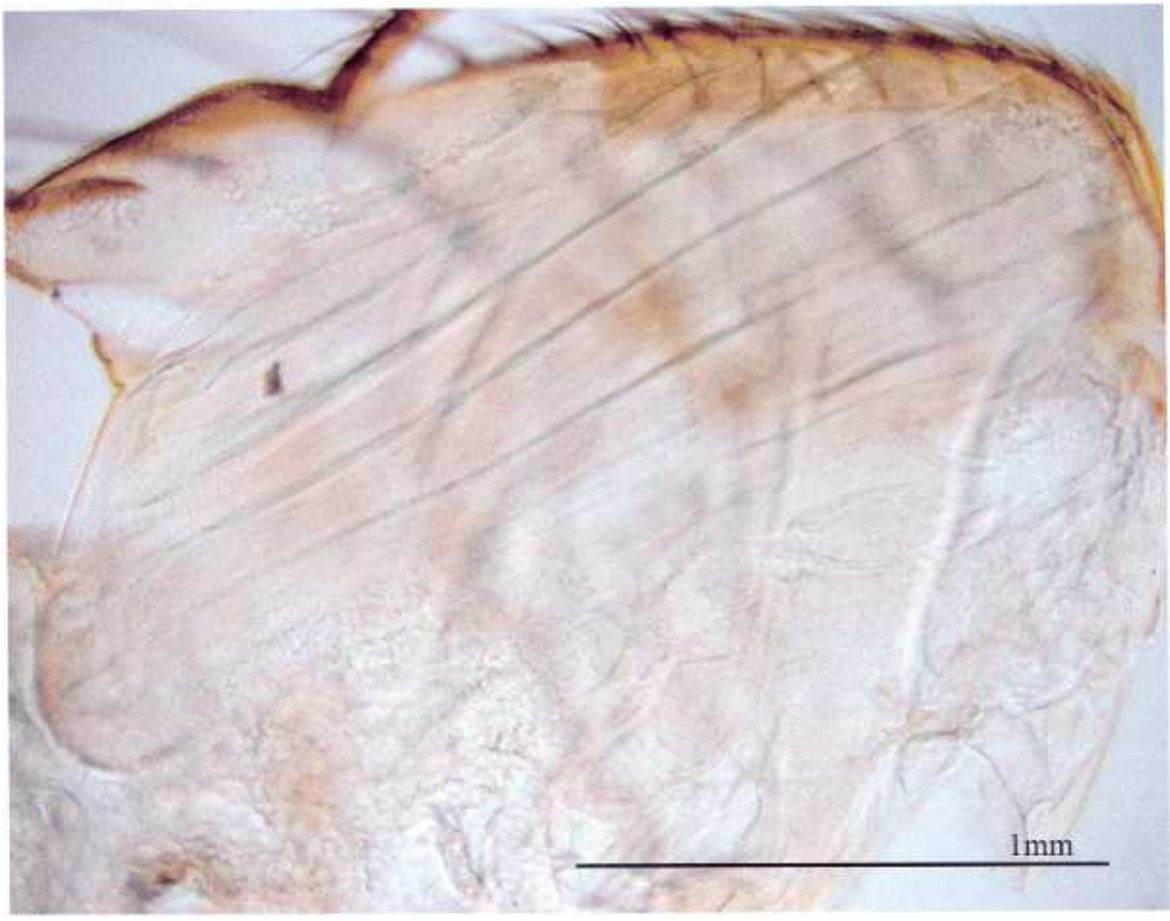

FIGURE 6. Mutant thorax bisection
The *C155 eag Sh; esg*^{EP} mutant thorax was bisected along the sagittal plane. A 1mm scale bar for 40x magnification is shown. The dorsal longitudinal muscles (DLM) are visible.

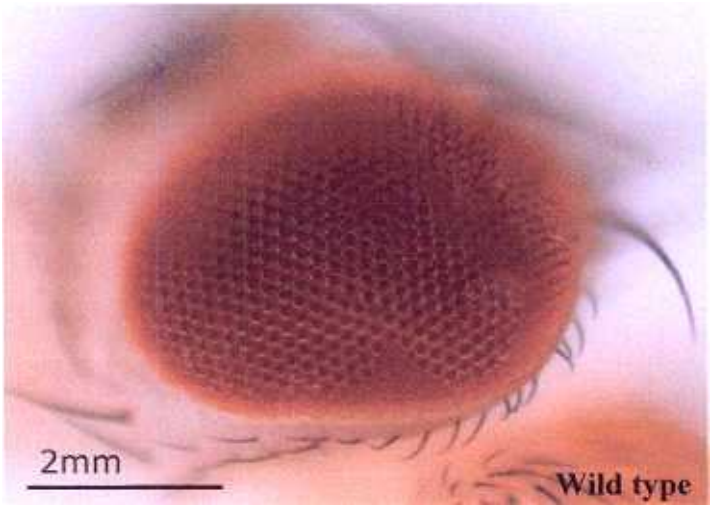

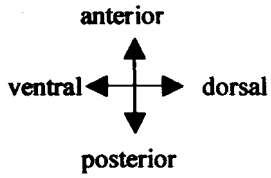

FIGURE 7. Eye phenotype The mutant specific eye phenotype of *C155 eag Sh; esg^{EP}* is compared to that of the wild type fly. A scale bar is shown for the magnification. The mutant eye consists of lower number of abnormally colored ommatidia, with bristles confined to the posterior-dorsal portion of the eye. Also note the stubby orbital bristles surrounding the mutant eye.

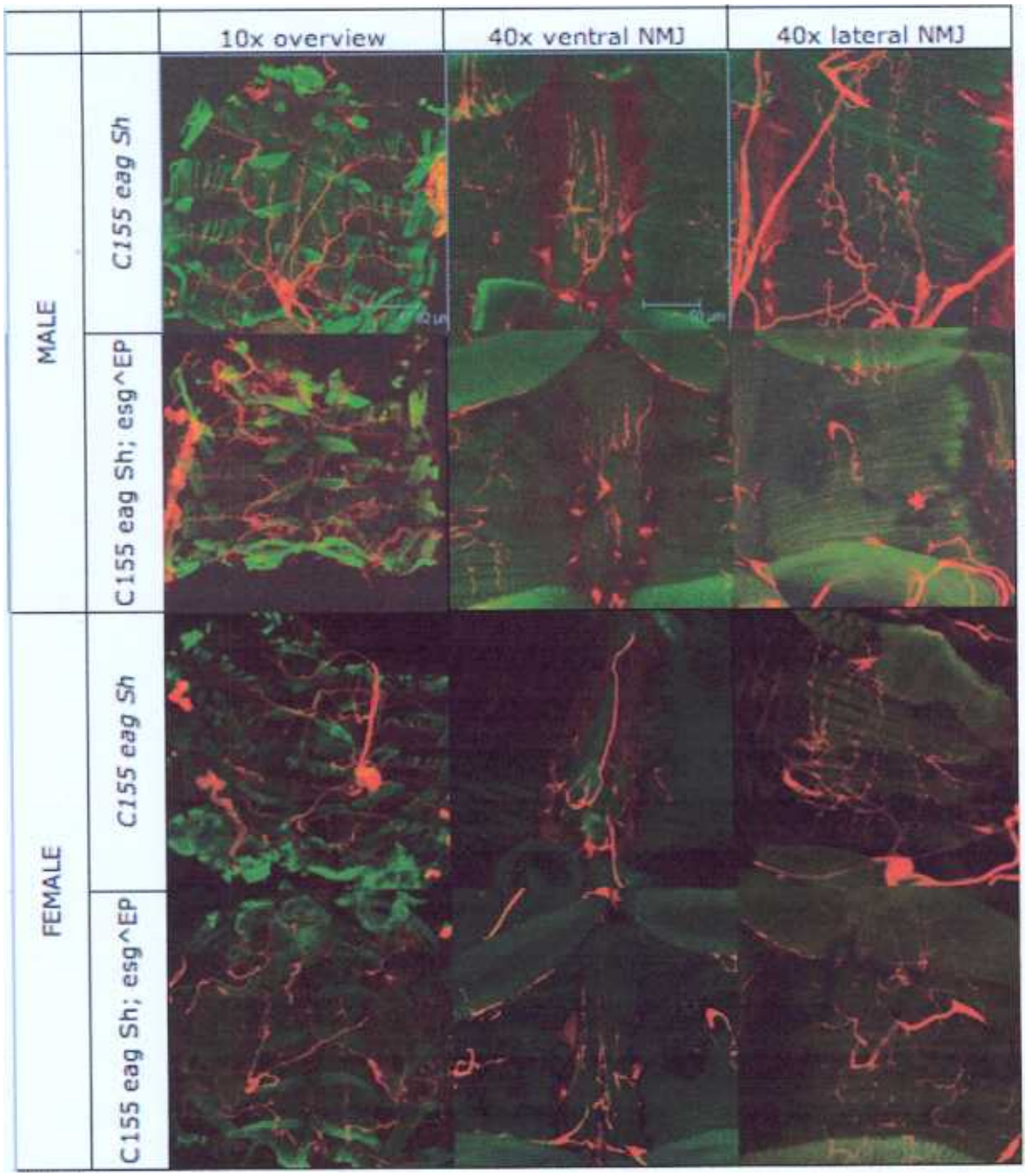

FIGURE 8. Adult abdominal NMJ
Confocal images show immunostaining of the NMJs of *eag Sh* and *C155 eag Sh; esg^{EP}* using phalloidin (green) and α-HRP (red). Scale bars are presented for the overview and the 40x magnifications. For the *C155 eag Sh; esg^{EP}* mutants, α-HRP labeled both the nerves and the muscles; to qualitatively compare synaptic development, the red α-HRP was accentuated over green with increased contrast. The ventral and lateral muscles were from the fourth abdominal segment. Note that in the lateral NMJ of C155 *eag Sh; esg^{EP}* mutant, there is a marked decreased in α-HRP specific labeling.

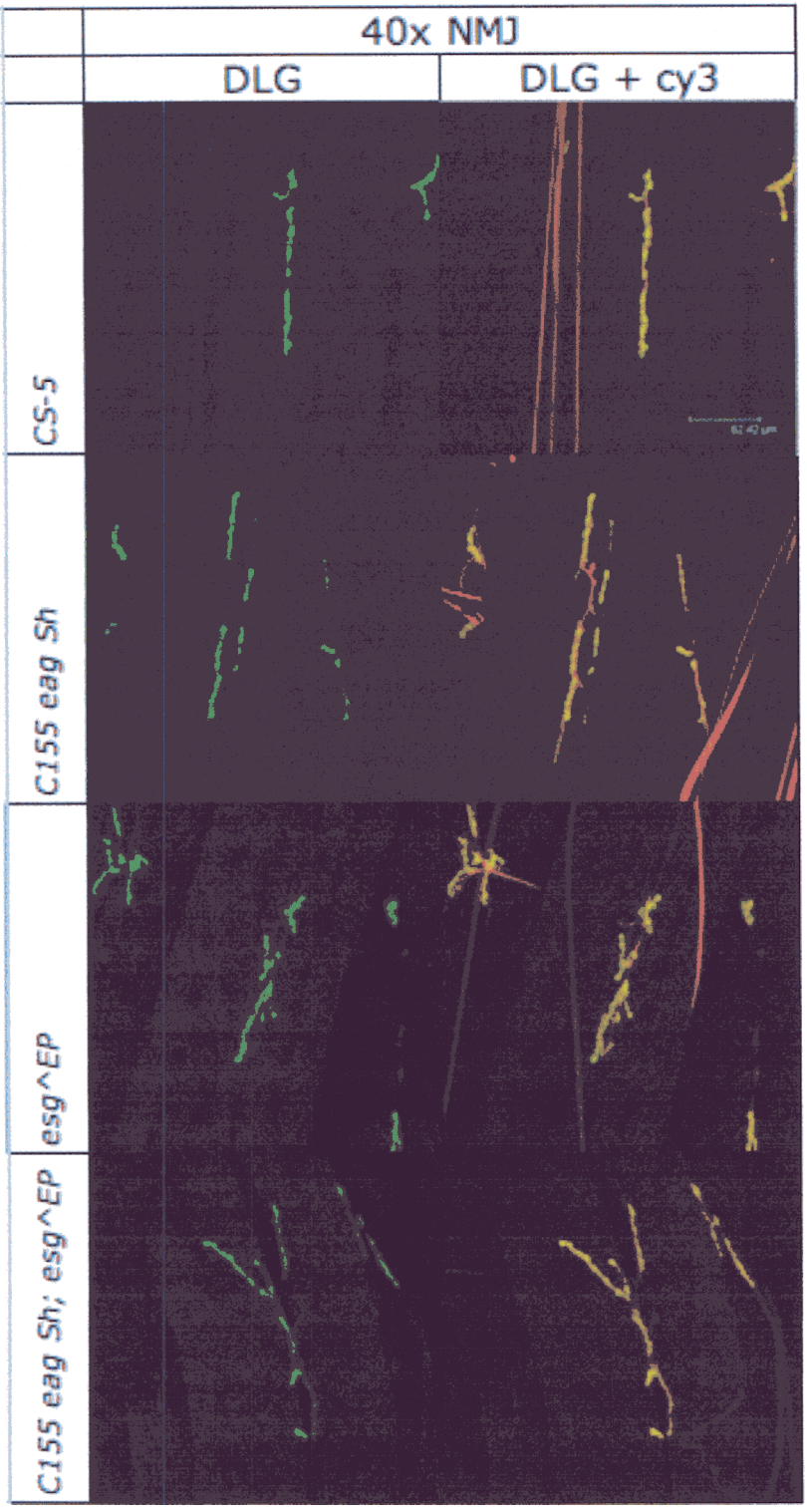

FIGURE 9. larval synaptic phenotype overview
Synaptic morphology is compared between mutants. Third-instar larval NMJs of were labeled with α-DLG (green) and α-HRP (red). The merged image is shown on the right. Scale bar is shown at 62.42um. Muscles 6 and 7 from the third segment are shown.

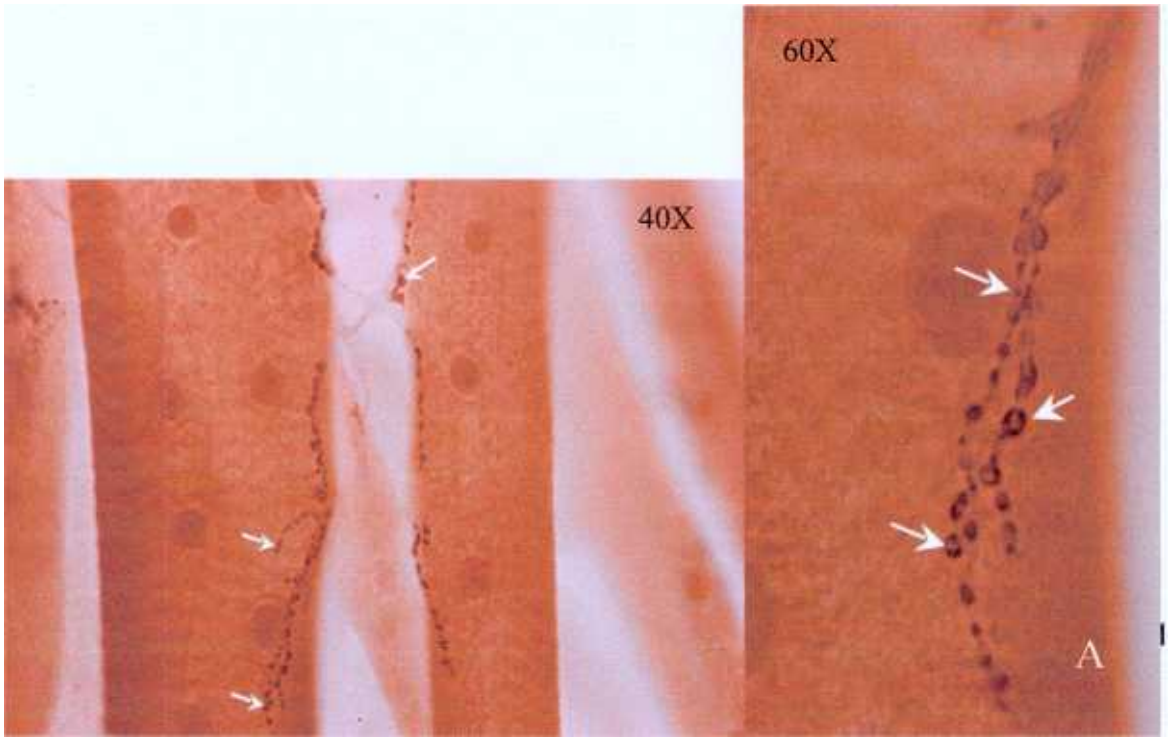

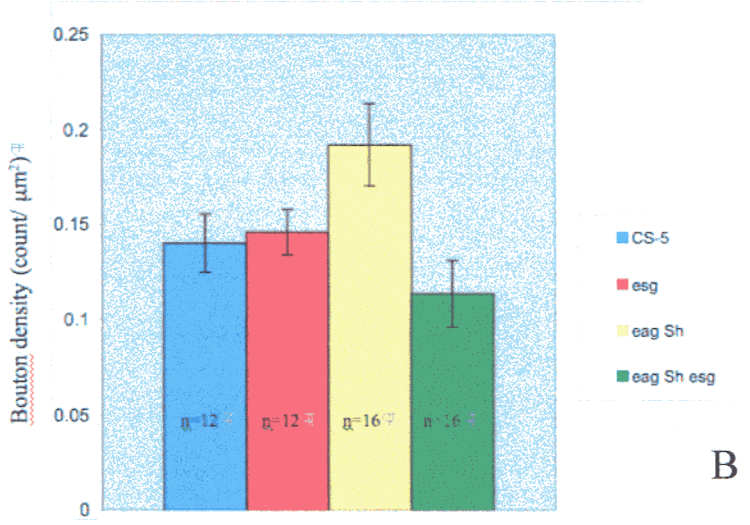

FIGURE 10.

A. DAB stained larvae prep of C155 *eag Sh; esg*^{EP}

Muscles 6 and 7 from the 4th segment of 3rd instar larvae were characterized at high magnification (shown 40x and 60x). For bouton specific labeling larval preps were incubated in primary antibody rabbit anti-synaptotagmin. Permanent staining was performed using DAB with ABC protocol. Note that boutons are of different size (arrow).

B. Bouton Densities of Larval NMJ

Bouton density was quantified from larval muscles 6 and 7 of the third segment. The preps were those of male third instar larvae. The difference between *C155 eag Sh; esg*^{EP} (n=16) and *C155 eag Sh* (n = 16) is significant ($p < 0.01$).

TABLES AND FIGURES

TABLE 1. *Drosophila* Stocks

Stock	Genotype
CS-5	*wildtype*
C155	*elav-Gal4^{C155}*
eag Sh	*eag Sh^{120}/ Fm7i-Bar, ubi-GFP*
EP(2)	*w; insertion^{EP} /Cyo or w; insertion^{EP} / insertion^{EP}*
esg^{EP}	*w; esg^{EP633}/ esg^{EP633}*
C155 eag sh	*elav-Gal4^{C155} eag Sh^{120}/ Fm7i-B GFP*
C155 eag sh; esg^{EP}	*elav-Gal4^{C155} eag Sh^{120}; esg^{EP633}*

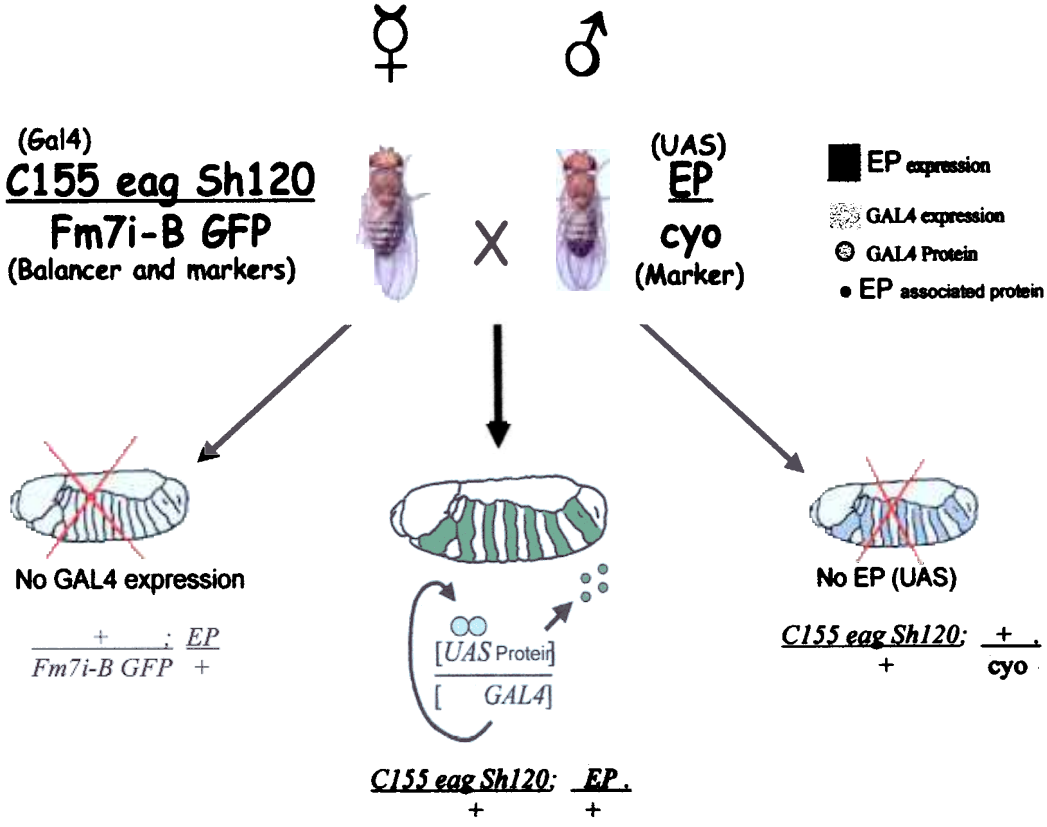

FIGURE 1. *C155 eag Sh* and *EP* cross

Virgin female flies carrying the recombinant X-chromosome *elav-gal4* ^{C155} *eag Sh* and the balancer chromosome, FM7i (which is marked with GFP and bar eyed) were crossed with males carrying a UAS-bearing EP insertion balanced over *Cyo* (*curly* marker). EP insertions on the second chromosome were examined in this study. Male F1 progeny that were hemizygous for *elav-Gal4*^{C155} *eag Sh* and contained one copy of UAS-bearing EP insertion were selected for study.

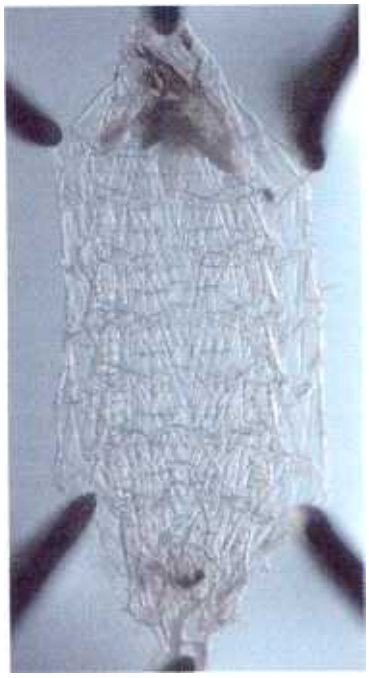

FIGURE 2. *Drosophila* larval prep
Third instar larvae were filleted in a magnetic dissecting dish. The prep was spread out as seen with magnetic pins. The larval muscles were visible along with the brain and ganglion located at the top of the prep.

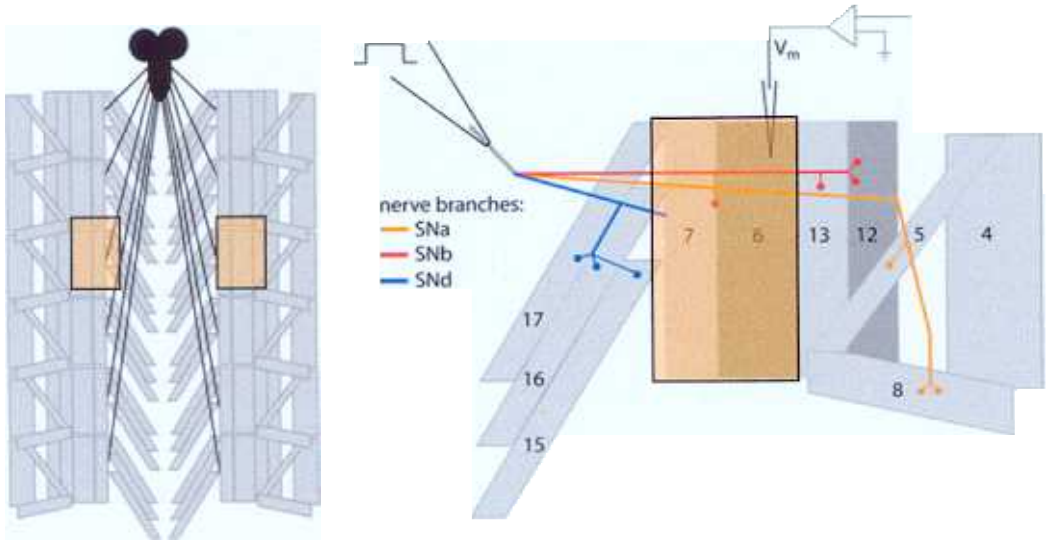

FIGURE 3. Larval muscle layout
Diagram of *Drosophila* larvae prep labels the muscles and perspective nerves that innervate each segment. For bouton density, boutons were counted from muscles 6 and 7 of the 3rd segment from the anterior end of the third instar wandering stage larvae (see colored segment).

From Hoy Lab website

TABLE 2. EP(2) screen

EP line suppressors	Gene	% survival	EP line lethals	Gene
EP(2)315	Unknown	65.5	EP627	Unknown
EP(2)316	Unknown	48.8	EP633	*escargot (esg)*
EP(2)330	Unknown	51.3	EP684	*escargot (esg)*
EP(2)337	GSTS1	80.5	EP2009	*escargot (esg)*
EP(2)340	Unknown	73.3		
EP(2)343	Unknown	47.5		
EP(2)348	Unknown	60.6		
EP(2)349	Unknown	50		
EP(2)354	lola	87.9		
EP(2)372	CG4738	54.4		
EP(2)397	chic	52		
EP(2)479	mef2	47		
EP(2)493	l(2)02045	51		
EP(2)531	CG13434	47		
EP(2)548	CG6751	44		
EP(2)608	E(Pc)	46		
EP(2)683	Unknown	41		
EP(2)938	Unknown	42		
EP(2)1236	GSTS1	47		

The results to date of the screen for second chromosome Enhancer P (EP(2)) mutations that suppress oxidative stress sensitivity of *eag Sh* are presented. The flies tested were males of genotype *elav-Gal4^{C155} eag Sh/y; EP/+*. They resulted from crosses between *elav-Gal4^{C155} eag Sh/FM7i-B GFP* virgin females and *w; EP/Cyo* males. Control flies of genotype *elav-Gal4^{C155} eag Sh/y* were used; after paraquat feeding, their mean percent survival was 14.9 ± 0.5% (n = 973). Suppressor lines were defined as crosses with mean percent survival ≥40%. Lethal lines were those that produced non-viable progeny in the cross. When known, the corresponding gene is noted.

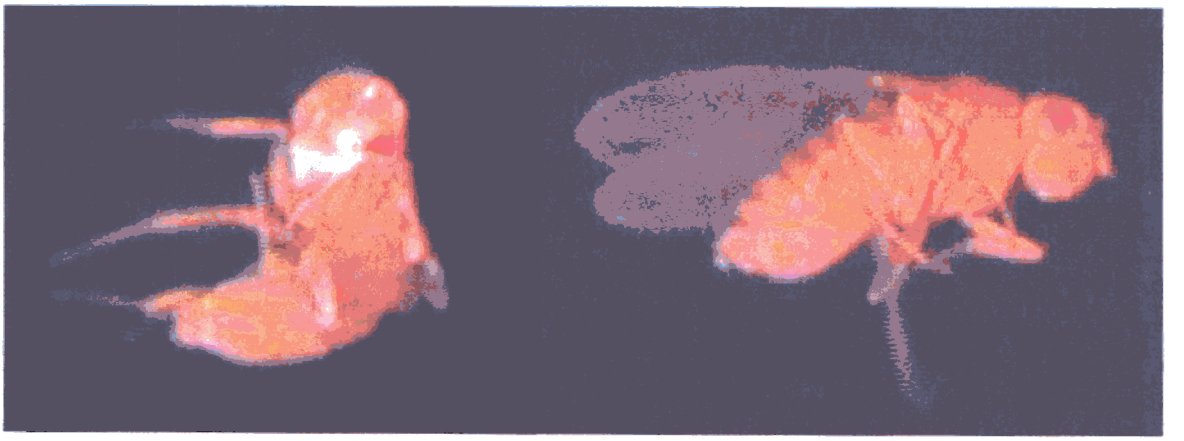

MALE
elav-Gal4^{C155} *eag Sh*^{120}*/Y; esg*^{EP633}*/+*

FEMALE
elav-Gal4^{C155} *eag Sh*^{120}*/+; esg*^{EP633}*/+*

FIGURE 4. C155 *eag Sh; esg*^{EP} adult
The adult mutant exhibits severe motor function impairments. The leg muscles of both male and female fly are contracted and shake in the absence of ether. These flies are unable to stand, and remain laying on their side or back. Their lifespan is about 48 to 72 hours after eclosion.

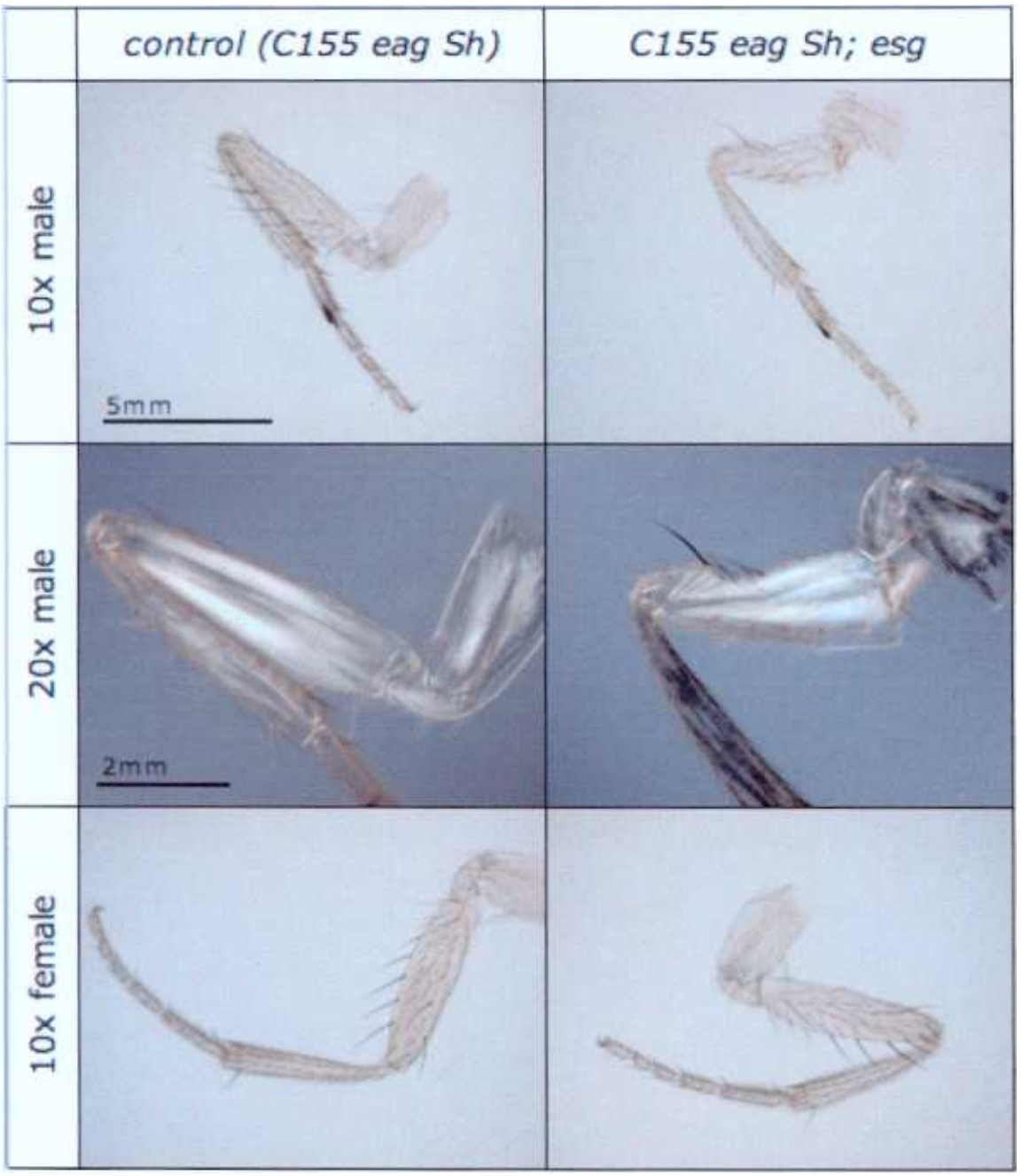

FIGURE 5. Mutant leg phenotype
Digital camera (10x) and stereoscope (20x) images of wild type and *C155 eag Sh; esg^{EP}* mutant legs are presented. Scale bars for 10x and 20x magnification are given. The control legs are those of *C155 eag Sh*, which exhibits wild type leg phenotype. The 10x image shows external bristles while the stereoscope image shows internal muscle structure.

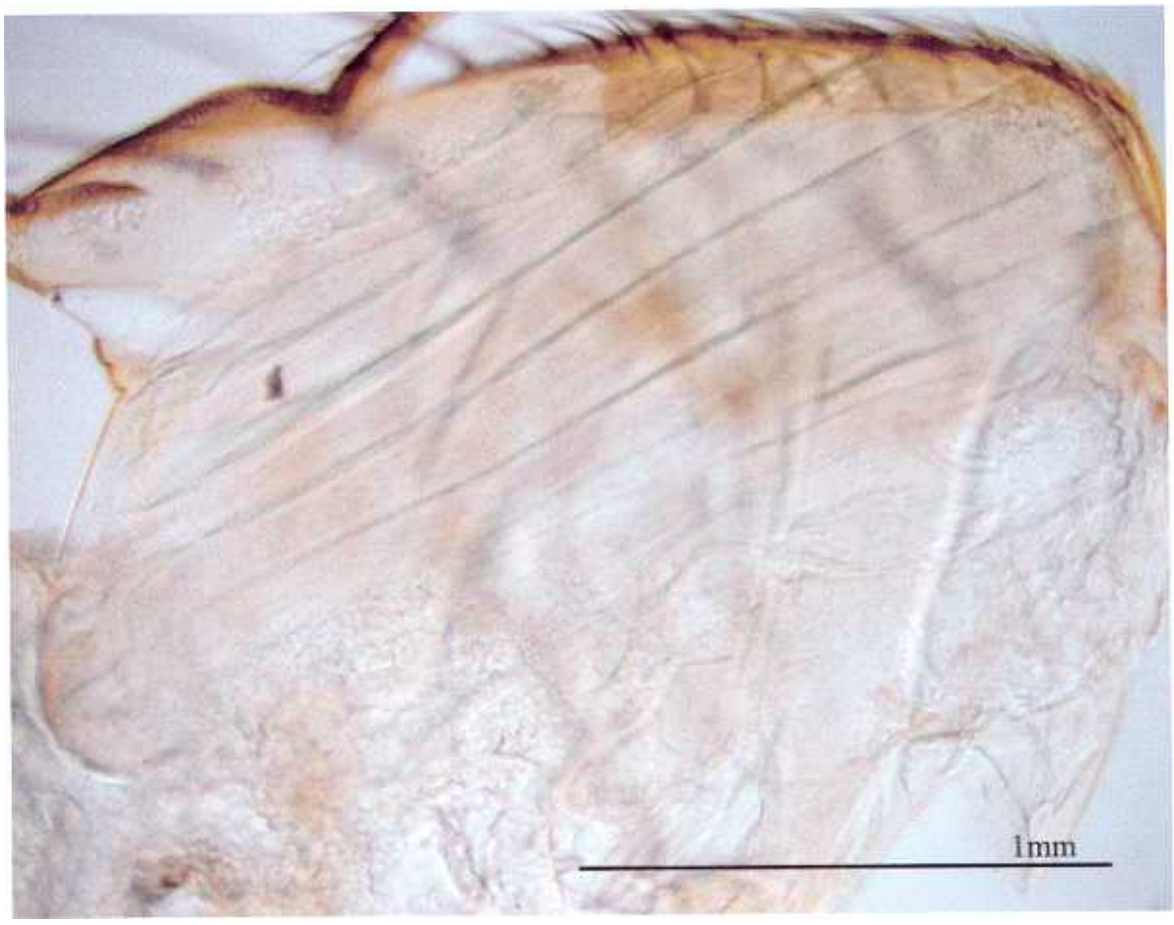

FIGURE 6. Mutant thorax bisection
The *C155 eag Sh; esg*^{EP} mutant thorax was bisected along the sagittal plane. A 1mm scale bar for 40x magnification is shown. The dorsal longitudinal muscles (DLM) are visible.

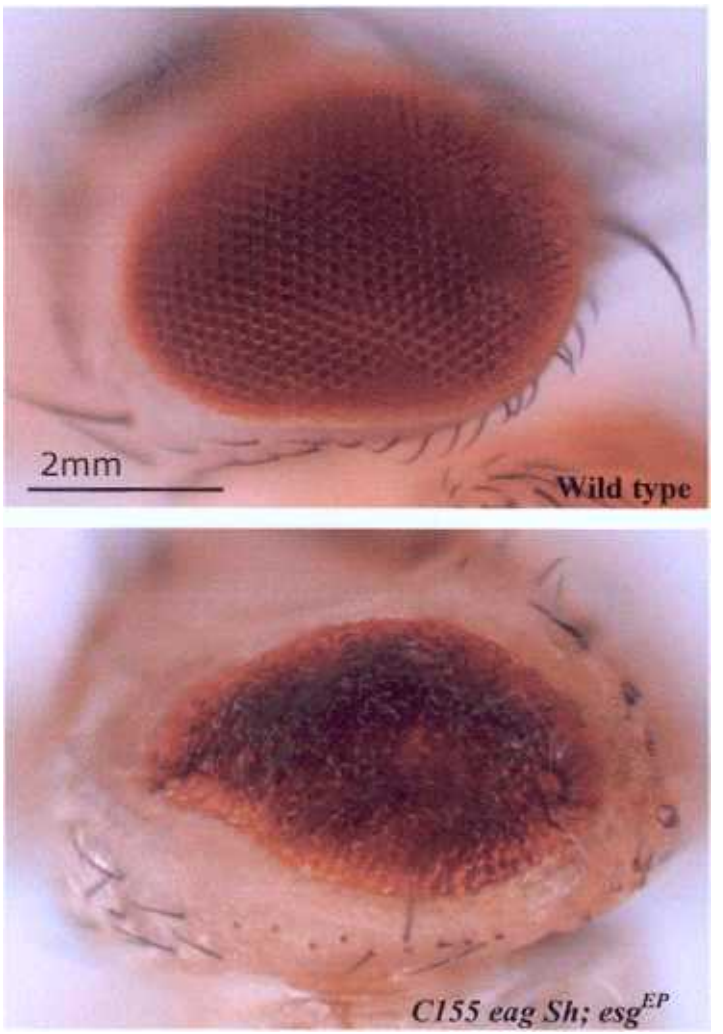

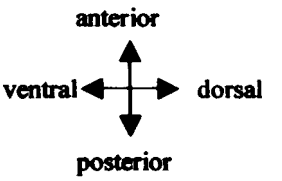

FIGURE 7. Eye phenotype The mutant specific eye phenotype of *C155 eag Sh; esg^{EP}* is compared to that of the wild type fly. A scale bar is shown for the magnification. The mutant eye consists of lower number of abnormally colored ommatidia, with bristles confined to the posterior-dorsal portion of the eye. Also note the stubby orbital bristles surrounding the mutant eye.

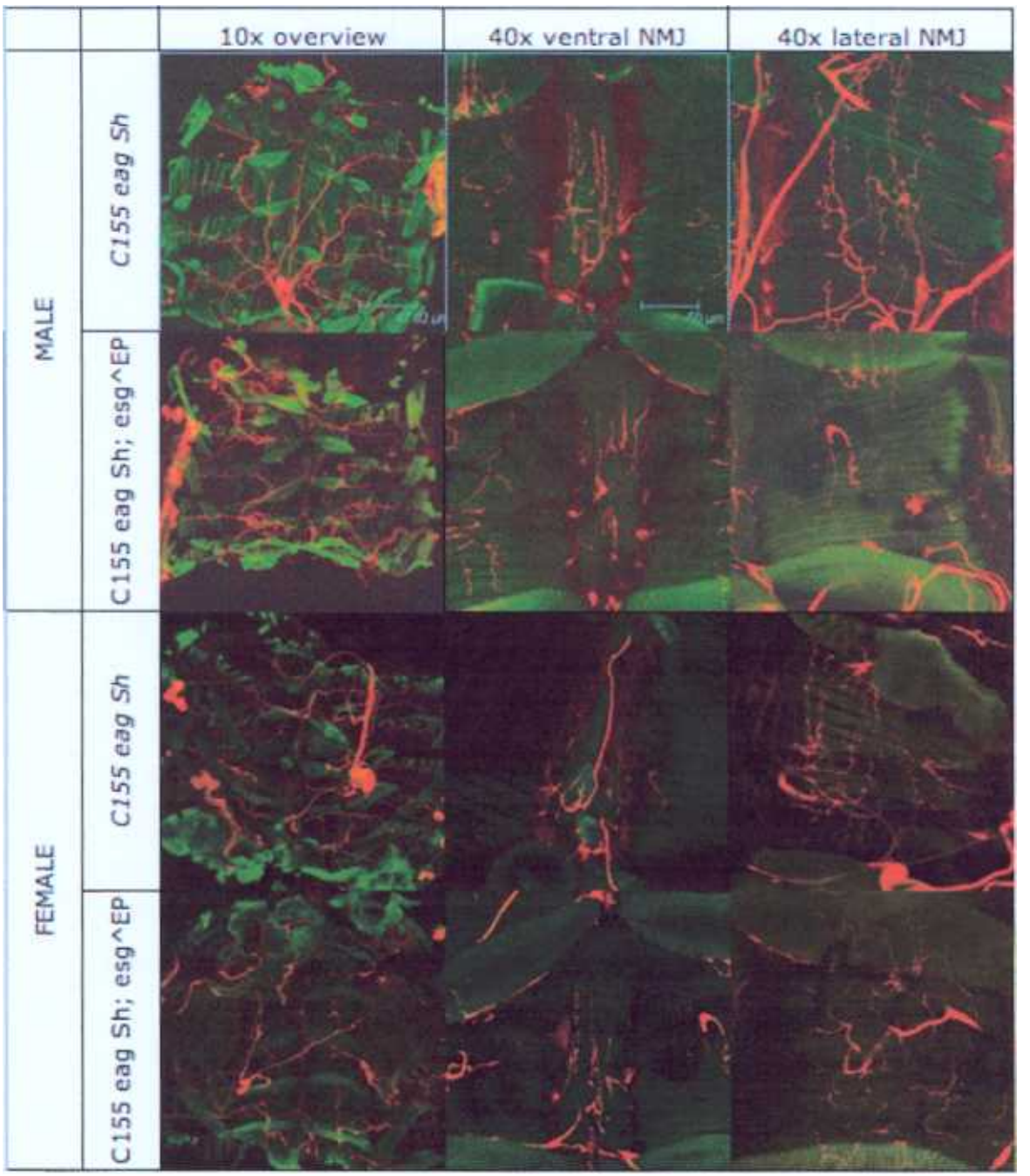

FIGURE 8. Adult abdominal NMJ
Confocal images show immunostaining of the NMJs of *eag Sh* and *C155 eag Sh; esg^{EP}* using phalloidin (green) and α-HRP (red). Scale bars are presented for the overview and the 40x magnifications. For the *C155 eag Sh; esg^{EP}* mutants, α-HRP labeled both the nerves and the muscles; to qualitatively compare synaptic development, the red α-HRP was accentuated over green with increased contrast. The ventral and lateral muscles were from the fourth abdominal segment. Note that in the lateral NMJ of C155 *eag Sh; esg^{EP}* mutant, there is a marked decreased in α-HRP specific labeling.

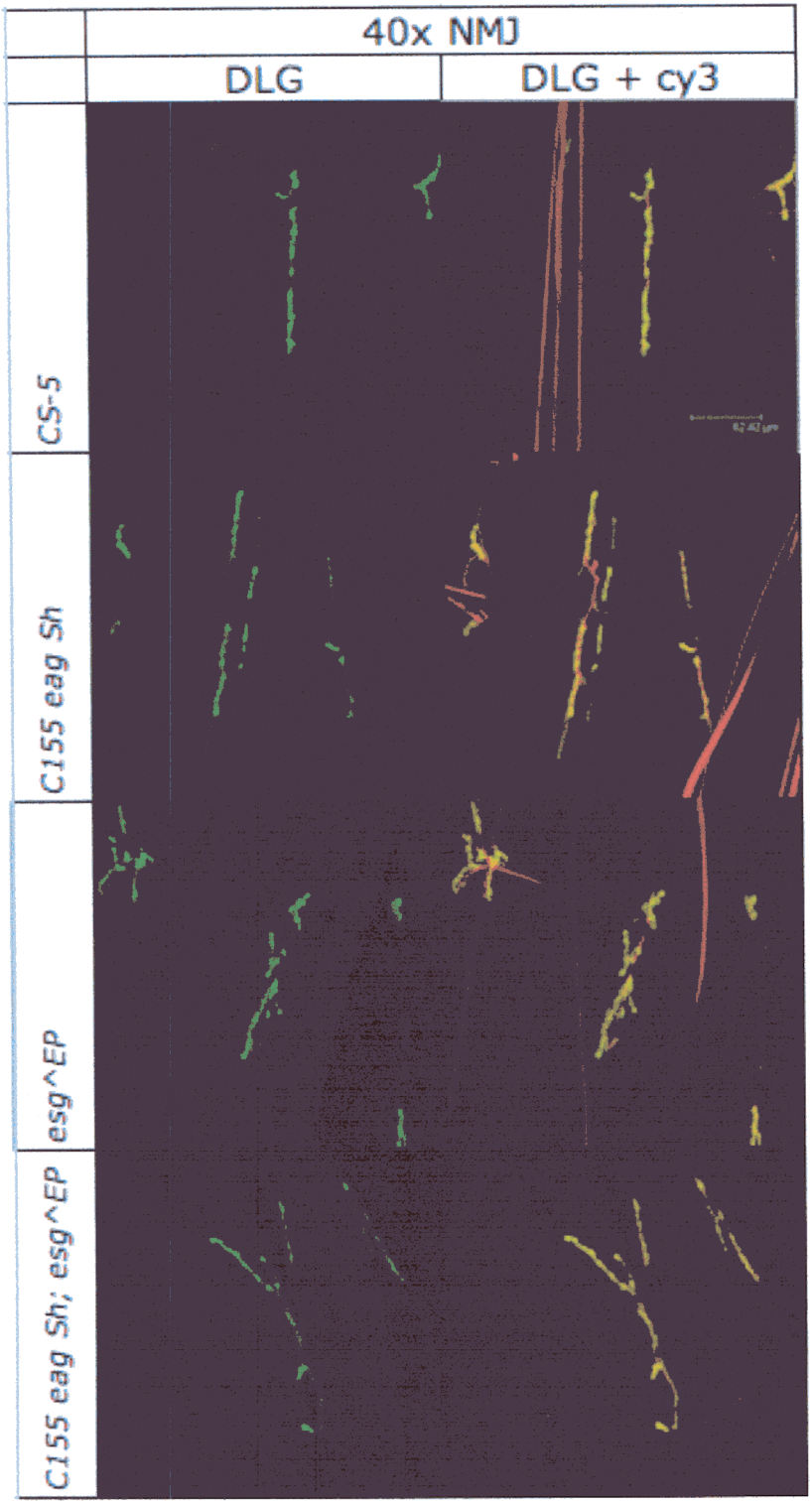

FIGURE 9. larval synaptic phenotype overview
Synaptic morphology is compared between mutants. Third-instar larval NMJs of were labeled with α-DLG (green) and α-HRP (red). The merged image is shown on the right. Scale bar is shown at 62.42um. Muscles 6 and 7 from the third segment are shown.

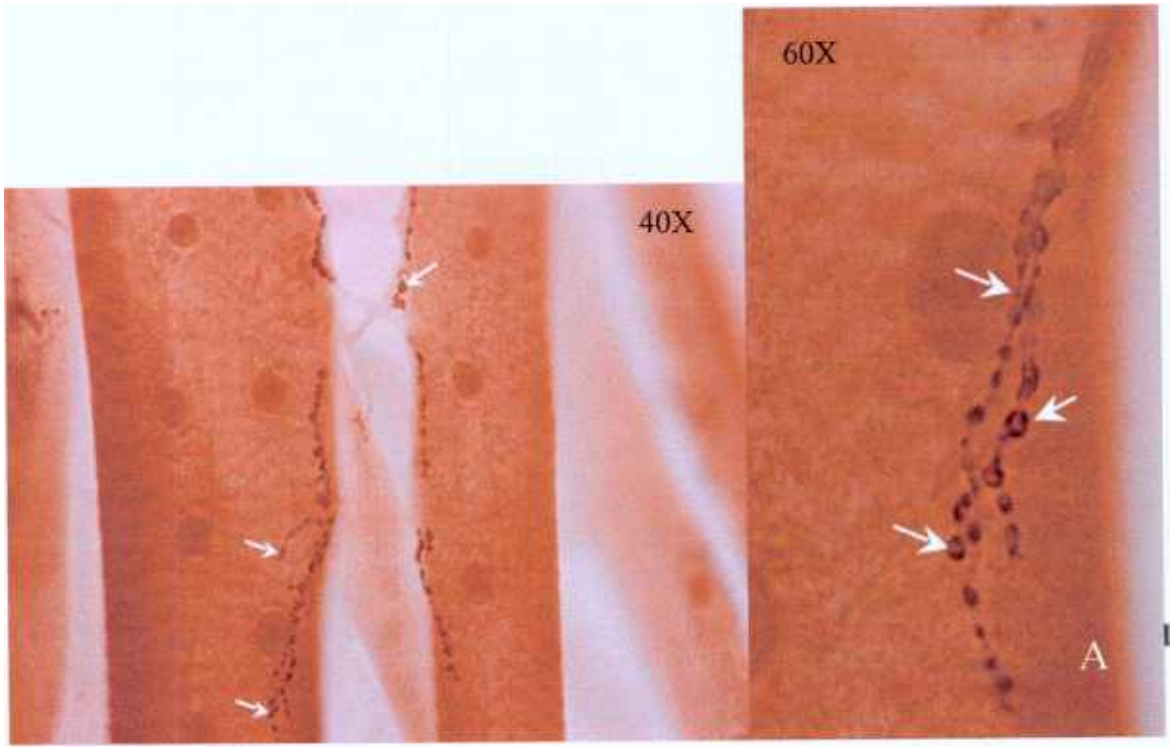

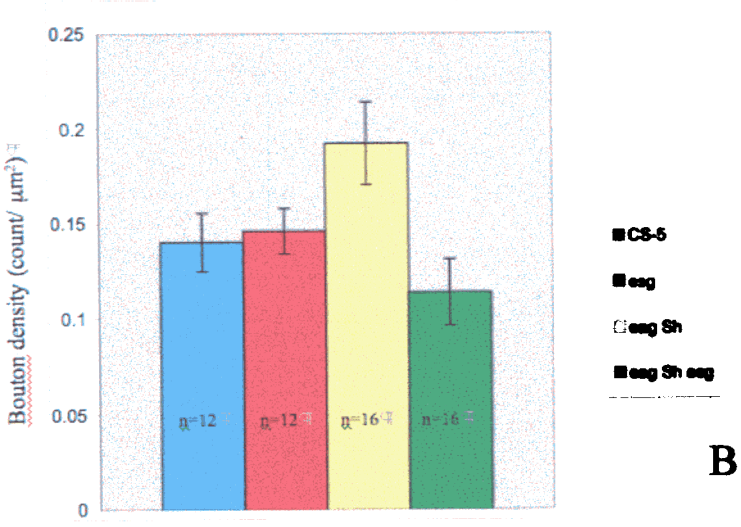

FIGURE 10.

A. DAB stained larvae prep of C155 *eag Sh; esg^{EP}*

Muscles 6 and 7 from the 4th segment of 3rd instar larvae were characterized at high magnification (shown 40x and 60x). For bouton specific labeling larval preps were incubated in primary antibody rabbit anti-synaptotagmin. Permanent staining was performed using DAB with ABC protocol. Note that boutons are of different size (arrow).

B. Bouton Densities of Larval NMJ

Bouton density was quantified from larval muscles 6 and 7 of the third segment. The preps were those of male third instar larvae. The difference between *C155 eag Sh; esg^{EP}* (n=16) and *C155 eag Sh* (n = 16) is significant ($p < 0.01$).